Catheterization and Cardiovascular Interventions 00:00–00 (2015)

Original Studies

Is High Pressure Postdilation Safe in Bioresorbable Vascular Scaffolds? Optical Coherence Tomography Observations after noncompliant Balloons Inflated at More than 24 Atmospheres

Enrico Fabris,[1,2] MD, Gianluca Caiazzo,[1] MD, PhD, Ismail Dogu Kilic,[1,3] MD, Roberta Serdoz,[1] MD, Gioel Gabrio Secco,[1,4] MD, Gianfranco Sinagra,[2] MD, Renick Lee,[5] BSC, Nicolas Foin,[5] PhD, and Carlo Di Mario,[1*] MD, PhD, FSCAI

Objectives: Optical coherence tomography (OCT) was used to investigate integrity and expansion of bioresorbable drug-eluting scaffolds (BVS) after high-pressure postdilation (HPPD). Background: Because of concerns about the risk of BVS damage, postdilation was not recommended and applied in the existing randomized studies and most registries. Recent real world data suggest incomplete BVS expansion cause higher rates of thrombosis. In vivo confirmation of the safety of high pressure postdilation is of paramount importance. Methods: Data from final OCT examination of consecutive implanted BVS, postdilated with noncompliant (NC) balloons at pressure $\geq$24 atm were analyzed. The following stent performance indices were assessed with OCT: mean and minimal lumen and scaffold area, residual area stenosis (RAS), incomplete strut apposition (ISA), tissue prolapse, eccentricity index (EI), symmetry index (SI), strut fractures, and edge dissections. Result: Twenty-two BVS postdilated at high pressure were analyzed. The average maximal postdilation balloon inflation (maxPD) was 28 ± 3 atm. High pressure OPN NC Balloon (SIS Medical AG, Winterthur Switzerland) was used in 41% of postdilations with a maximal PD of 30 ± 4.7 atm. Final mean and minimal lumen area were 6.8 ± 1.4 and 5.5 ± 1.4 mm^2, respectively. OCT showed low percentage of RAS (16 ± 9.6%), and low percentage of ISA (1.8 ± 2.4%). Mean EI was 0.86 ± 0.02 and SI 0.35 ± 0.14. OCT analysis showed one edge dissection and no scaffold fractures. Conclusions: BVS deployment optimization using HPPD does not cause BVS disruption and is associated with a good BVS expansion, low rate of strut malapposition and edge dissections.

Key words: bioresorbable vascular scaffolds; optical coherence tomography; noncompliant balloon; struts apposition; coronary angioplasty

[1]NIHR Biomedical Research Unit, Royal Brompton and Harefield NHS Foundation Trust, London, United Kingdom
[2]Cardiovascular Department, Ospedali Riuniti and University of Trieste, Trieste, Italy
[3]Department of Cardiology, Pamukkale University, Denizli, Turkey
[4]Department of Clinical and Experimental Medicine, University of Eastern Piedmont, Novara, Italy
[5]National Heart Centre Singapore, Singapore

Conflict of interest: Nothing to report.

*Correspondence to: Carlo Di Mario, MD, PHD, FACC, FSCAI, FESC, FRCP, NIHR Cardiovascular BRU, Royal Brompton Hospital, Sydney Street, London SW3 6NP, United Kingdom. E-mail: c.dimario@rbht.nhs.uk

Received 16 December 2014; Revision accepted 9 August 2015

DOI: 10.1002/ccd.26222
Published online 00 Month 2015 in Wiley Online Library (wileyonlinelibrary.com)

INTRODUCTION

Stent under expansion might result in an increased risk of in-stent restenosis and thrombosis [1] so that optimization of the expansion of the deployed stent still represent a critical issue during percutaneous coronary intervention.

Bioreasorbable drug-eluting scaffolds (BVS) (ABSORB, Abbott Vascular, Santa Clara, California) have emerged as a potential major breakthrough for treatment of symptomatic coronary artery lesions showing unique potential in vascular repair with restoration of vasomotion, reduction of plaque thickness, and compensatory enlargement leading to late lumen enlargement [2–5].

BVS have become widely available and their use for treatment of complex lesions is also increasing worldwide. However, the mechanical properties of these polymer-based scaffolds substantially differ from those of metal stents and the relatively lower radial strength may result in insufficient scaffold expansion. For this reason, optimal preparation of the lesion before deployment received great emphasis [2,6]; conversely, aggressive postdilation of BVS was not recommended because of the risk of scaffold fracture [5]. In recent registries, the indications for BVS implantation were expanded to complex coronary lesions [7,8] and the presence of higher than expected rates of scaffold thrombosis highlights the importance of BVS postdilation [9].

In vivo data on scaffold integrity after high-pressure postdilation (HPPD) are not yet available. Aim of this study was the assessment of the acute performance of BVS after HPPD and extremely HPPD using optical coherence tomography (OCT).

MATERIALS AND METHODS

Study Population

The study population comprised consecutive patients undergoing BVS implantation under OCT guidance, which is our routine for scaffold deployment, and in which deployment optimization was achieved using HPPD ($\geq$24 atm) with noncompliant (NC) balloons or OPN NC balloon (SIS Medical AG, Winterthur, Switzerland). From September 2012 until August 2014, 103 BVS were implanted in 80 lesions of 62 patients at the Royal Brompton Hospital (London, United Kingdom). We identified 22 BVS that were post dilated with HPPD in 20 lesions of 16 patients. A final OCT run was performed to assess post deployment scaffold characteristics. BVS were not used in patients presenting with acute ST-segment elevation myocardial infarction, coronary bifurcations with a default 2-stent strategy, an estimated glomerular filtration rate $<$30 ml/min, and aorto-ostial lesions. All patients signed a written informed consent for percutaneous coronary intervention and OCT guidance as part of the general consent.

Treatment Procedures

All lesions were treated with predilation using conventional semicompliant or NC balloons. The use of additional devices (cutting balloons or rotablator) was left to the operator's discretion. Deployment of the BVS was performed using slow balloon inflation (i.e., 2 atm per 10 s) without exceeding the rated pressure indicated in the product instructions for use. OCT assessment was performed in most cases before stent deployment for BVS sizing and repeated when stent expansion was considered optimal angiographically. In some cases of suboptimal deployment as assessed with OCT, further postdilation was performed after which a final OCT scan was performed and used for the study analysis.

Quantitative Coronary Angiography Analysis and Lesion Characterization

Quantitative coronary angiography (QCA) was performed off line after the procedure using a computer-based QCA system (CAASQCA-2D system, Pie Medical Imaging BV, Maastricht, the Netherlands) with the dye-filled catheter used for calibration. For each lesion, the following QCA parameters were measured: minimal lumen diameter, reference vessel diameter (RVD), percentage area stenosis, and lesion obstruction length. The largest balloon diameter and maximal inflation pressure during lesion predilatation were recorded and used to calculate the balloon/artery ratio (mean inflated balloon diameter/mean reference vessel diameter). In addition, we qualitatively assessed the presence of angiographic calcification from absent to severe.

OCT Assessment

Frequency domain OCT was performed using the C7 system or the Ilumien Optis system (St. Jude Medical, Minneapolis, Minnesota). For both systems, DragonFly or DragonFly 2 imaging catheters (St. Jude Medical) were used. Automatic pullbacks were performed at 20 mm/s during contrast injection at a rate of 3–5 ml/s using a power injector. The OCT catheter was inserted distal to the treated segment, and the pullback continued until either the guiding catheter was reached or the maximal pullback length (5.5 cm with the C7 system and 7.4 cm with the Ilumien Optis system) was completed. Two sequential pullbacks were combined to

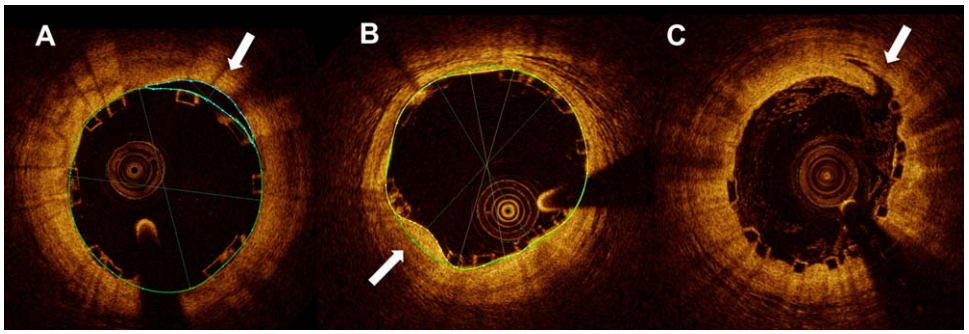

Fig. 1. (A) An example of incomplete strut apposition (ISA) (arrow). There are 2 malapposed struts between 12 and 2 o'clock position. In a bioresorbable vascular scaffold (BVS), the possibility of identifying the abluminal border of the struts allows evaluation of the ISA area. (B) An example of tissue prolapse (arrows). The prolapse area was measured as the difference between the stent and lumen area as shown in the figure. (C) An example of edge dissection (arrows). [Color figure can be viewed in the online issue, which is available at wileyonlinelibrary.com.]

enable assessment of the entire stented segment when required.

OCT Offline Analysis

The OCT measurements were repeated offline using the LightLab Imaging workstation (St. Jude Medical). The analysis of contiguous cross sections was performed at 1 mm intervals within the entire stented segment and at 5 mm proximal and distal to the BVS edges to measure the proximal and distal reference vessel area (RVA) and to identify dissections. RVA was calculated as the mean of the two largest luminal areas 5 mm proximal and distal to the BVS edge[10]. In case of the absence of a meaningful proximal or distal segment (bifurcations, poststenotic aneurysm, and so on) only a proximal or distal reference cross section was used to calculate the RVA [11]. Edge dissection was defined as a disruption of the vessel wall in the 5 mm proximal or distal to the stent edge with visible flap (see Fig. 1). Stent fracture was suspected in the presence of isolated struts lying unapposed in the lumen with no connection or overridden by the contiguous stent struts. Suspicious cases were sent for 3D reconstruction. For each cross section analyzed, the area and the mean, maximal, and minimal diameter of the scaffold were automatically contoured and measured by the analysis system, with manual correction as appropriate [6]. Incomplete strut apposition (ISA) was defined as presence of struts separated from the underlying vessel wall [10] (see Fig. 1). Tissue prolapse was defined as the presence of tissue protruding between stent struts extending into the lumen as a circular arc connecting adjacent struts [6] (see Fig. 1). The following quantitative parameters were calculated for each scaffold [2,10,12,13]: the percentage of the ISA, calculated as a ratio of unopposed struts and total number of struts at 1 mm intervals. ISA area and tissue prolapse area were also measured. Percentage residual area stenosis (RAS) was calculated as: [1 − (minimal lumen area/RVA) × 100]. The eccentricity index was calculated as the ratio between minimal and maximal in-stent diameter[14]. The symmetry index was defined as: (maximal stent diameter−minimal stent diameter)/(maximal stent diameter) [10].

Statistical Analyses

Summary statistics of clinical and procedural variables were expressed as mean and standard deviation or median and interquartile range or counts and percentage, as appropriate.

The entire analysis was performed using the IBM SPSS package version 19.

RESULTS

In the 24-month study period, we identified 22 BVS that were deployed in 20 lesions of 16 patients and postdilated with a maximal balloon inflation pressure of 28.0 ± 3.8 atm (range 24–40 Atm).

Baseline clinical characteristics are shown in Table I. Angiographic and QCA baseline lesion characteristics are summarized in Table II. The left anterior descending artery was the target vessel in the majority of cases (55%). Most lesions were complex (B2+C = 70%) according to the American College of Cardiology/American Heart Association classification criteria.

As shown in Table III the balloon to artery ratio (balloon diameter/mean reference vessel diameter ratio) for predilation was 1.08 ± 0.2. Cutting balloon was used in 9% of cases. The median stent length was

TABLE I. Patient Characteristics

Patient characteristics ($n = 16$)	
Age, yrs	59 ± 10
Male sex	14 (87.5%)
Hypertension	11 (68.8)
Hypercholesterolemia	12 (75%)
Diabetes	3 (18%)
Current smokers	4 (25%)
Previous PCI	4 (25%)
Previous myocardial infarction	6 (37%)
Previous CABG	0
Previous stroke	1 (6.25%)
History of chronic kidney disease	2 (12.5%)
Creatinine, μmol/L	78 ± 20
LV ejection fraction, %	51 ± 9
Clinical indication	
Stable angina	15 (93.8)
Unstable angina	1 (6.3%)
Number of diseased vessels	
1	10 (62.5%)
2	6 (37.5%)

Values are *n* (%), or mean ± SD.
CABG, coronary artery bypass graft; LV, left ventricular; PCI, percutaneous coronary intervention; yrs, years.

TABLE II. Angiographic and QCA Lesion Characteristic ($n = 20$)

Angiographic and QCA lesion characteristic ($n = 20$)	
Target vessel	
LAD	11 (55%)
DIAGONAL	2 (10%)
LCX	2 (10%)
RCA	5 (25%)
AHA/ACC lesion classification	
B1	6 (30%)
B2	3 (15%)
C	11 (55%)
Bifurcation	4 (20%)
Moderate to heavy calcification[a]	7 (35%)
QCA analysis	
RVD, mm	2.69 ± 0.43
MLD, mm	0.87 ± 0.32
AS, %	83.6 ± 7.5
DS, %	67.8 ± 6.7
Length mm	17.5 ± 8.4

Values are *n* (%) or or mean ± SD.
AS, area stenosis; DS, diameter stenosis; LAD, left anterior descending artery; LCX, left circumflex artery; MLD, minimal lumen diameter; QCA, quantitative coronary angiography; RCA,right coronary artery; RVD, reference vessel diameter.
[a]Angiographic assessment of the degree of calcification.

28 mm [interquartile range (IQR) 18–28] and the median stent diameter was 3 mm (IQR 2.9–3.5). Median maximal postdilation balloon diameter was 3.0 mm (IQR 3.0–3.5). Post dilation balloon/Scaffold diameter ratio was 1.02 ± 0.11.

High pressure OPN NC Balloons (SIS Medical AG, Winterthur, Switzerland) were used in 41% of postdilations with maximal inflation pressure of 30 ± 4.7 atm.

TABLE III. Procedural Characteristics

Procedural characteristics	
Maximal diameter balloon predilation, mm	2.5 (2.5–2.62)
Maximal predilation balloon inflation, atm	19.6 ± 6
Balloon/artery ratio	1.08 ± 0.2
NC balloon predilation	22 (100%)
Cutting balloon predilation	2 (9%)
Scaffold diameter, mm	3.0 (2.9–3.5)
Scaffold length, mm	28 (18–28)
Maximal postdilation balloon diameter, mm	3.0 (3.0–3.5)
Use of NC postdilation balloon with diameter of 3.5	9 (41%)
Use of NC postdilation balloon with diameter of 3.0	9 (41%)
Use of NC postdilation balloon with diameter of 2.5	4 (18%)
Maximal postdilation balloon inflation, atm	28 ± 3.8
Postdilation balloon/Scaffold diameter ratio	1.02 ± 0.11
Use of OPN NC Balloon	9 (41%)

Values are *n* (%), mean ± SD or median (interquartile range 25–75).
NC, non compliant; OPN, "OPN NC Balloon (SIS Medical AG, Winterthur Switzerland)."

TABLE IV. Optical Coherence Tomography Findings

Optical Coherence Tomography Findings	
BVS (n 22)	
Mean scaffold area, mm^2	$6.83 \pm 1{,}42$
Minimal scaffold area, mm^2	5.57 ± 1.45
Mean lumen area, mm^2	6.79 ± 1.4
Minimal lumen area, mm^2	5.54 ± 1.43
Mean scaffold diameter, mm	2.9 ± 0.31
Minimal scaffold diameter, mm	2.7 ± 0.28
Maximal scaffold diameter, mm	3.1 ± 0.36
Percentage RAS	$16 \pm 9.6\%$
Stent with RAS >20%	8 (36%)
Mean eccentricity index	0.86 ± 0.02
Minimum eccentricity index	$0.72 \pm 0{,}1$
Symmetry index	0.35 ± 0.14
ISA analysis	
Percentage of malapposed struts	1.84 ± 2.4
Scaffold without any ISA	7 (32%)
Scaffold with ISA at the proximal edge	7 (32%)
Scaffold with ISA at the distal edge	6 (27%)
ISA area, mm^2	0.46 ± 0.9
Maximal ISA length, mm	0.21 ± 0.2
Prolapse area, mm^2	1.33 ± 1.8
Edge dissection	1 (4.5%)
Scaffold Fractures	0

Values are *n* (%) or mean ± SD.
ISA, incomplete strut apposition; RAS, residual area stenosis.

OCT findings are summarized in Table IV. A total of 736 cross sections and 4875 struts were analyzed. The mean and minimal lumen areas were 6.8 ± 1.4 and 5.5 ± 1.4 mm^2, respectively. RAS was $16 \pm 9.6\%$ and RAS >20% was present in 36% of scaffolds. OCT showed $1.84 \pm 2.40\%$ malapposed struts and scaffolds without any ISA were 32%. There was no difference between ISA at the proximal edge and ISA at the distal edge (32% vs. 27% $P = 0.7$). The mean and minimal eccentricity index and symmetry index were 0.86 ± 0.02, 0.72 ± 0.1, and 0.35 ± 0.14, respectively. Mean prolapse

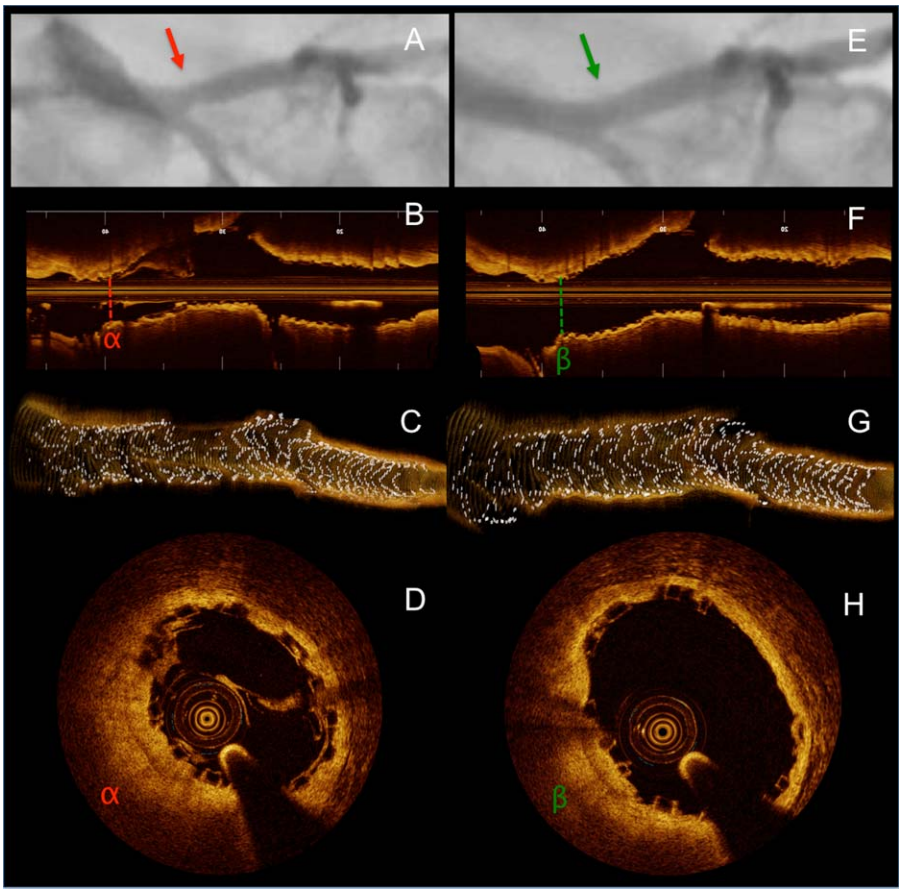

Fig. 2. An example of BVS deployment optimization with HPPD. (A) angiographic result after deployment in the proximal LAD of a 3.0 × 28 mm BVS Absorb and postdilated with a 3.5 mm NC balloon to 16 atm. It clearly visible a narrowing within the scaffold in the ostial LAD. (B) OCT long view image confirming the under expansion of the scaffold in the proximal part (red arrow). (C) OCT three-dimensional reconstruction of BVS using ImageJ software. (D) OCT cross sectional area (α) showing under expansion of the scaffold before HPPD, lumen area: 4.53 mm^2, mean diameter: 2.38 mm, minimal diameter: 2.05 mm, maximal diameter: 2.83 mm. (E) Final angiographic result after HPPD with a 3.5 × 8 mm NC balloon to 28 atm showing absence of narrowing. (F) OCT long view after HPPD. It is evident the better scaffold expansion. (G) OCT three-dimensional reconstruction of BVS showing integrity and good expansion of the scaffold. (H) OCT cross sectional area (β), matched with α cross sectional area after HPPD showing optimal scaffold expansion: lumen area: 7.71 mm^2, mean diameter: 3.01 mm, minimal diameter: 2.67 mm, maximal diameter: 3.45 mm. HPPD, High pressure post dilation; LAD, left anterior descending artery; OCT, optical coherence tomography. [Color figure can be viewed in the online issue, which is available at wileyonlinelibrary.com.]

area was 1.33 ± 1.8 mm^2. OCT analysis showed only 1 edge dissection (4.5%) and no scaffold fractures.

DISCUSSION

This study is the first to address the acute performance of BVS after high pressure and extremely HPPD.

The effect of HPPD on BVS was evaluated with OCT which allows for more accurate detection and quantification of scaffold integrity, malapposition, underexpansion, tissue prolapse, and scaffold edge dissections, when compared with conventional intravascular imaging modalities [15,16]. Moreover, the OCT indices used in our study are widely accepted as criteria for the evaluation of stent deployment [10,13].

We showed for the first time that BVS deployment HPPD optimization is feasible and safe. Optimal stent expansion and strut apposition using HPPD strategy were achieved without any scaffold fracture or significant vascular damage. Considering also the presence of complex lesion subset, final OCT evaluation showed low percentage of ISA ($1.84 \pm 2.4\%$), as well as low percentage of scaffolds with at least one ISA (68%), of RAS ($16 \pm 9.6\%$) and of RAS>20% (36%). A recent substudy of ABSORB cohort B showed that, despite the much lower complexity, 75% of lesions had at least one malapposed strut and the mean ISA was 6.2%, a

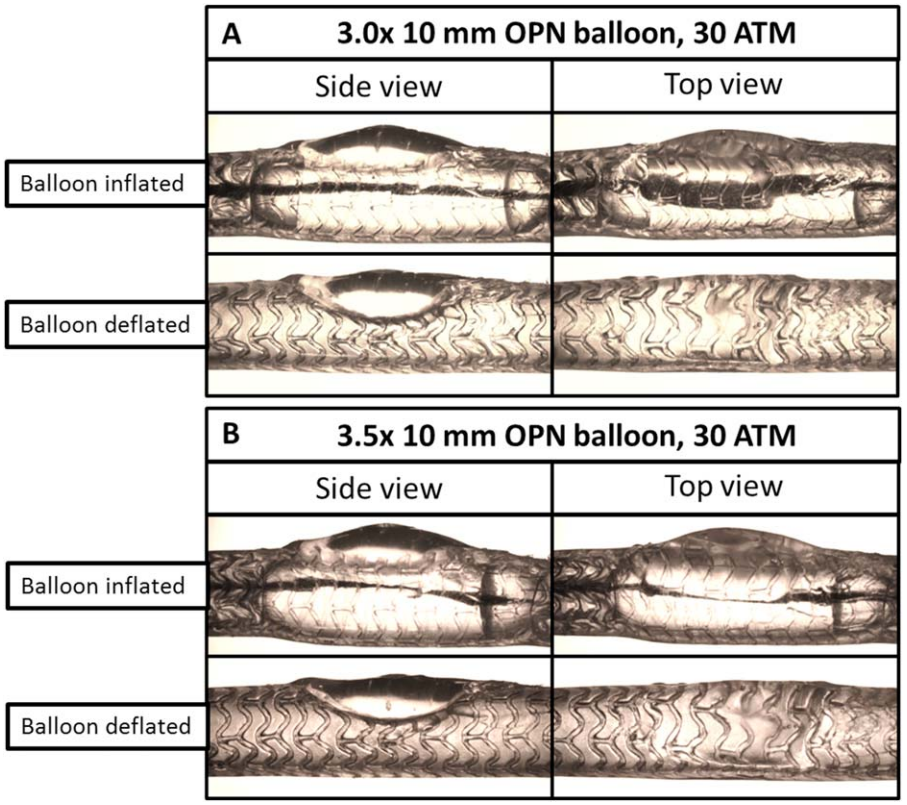

Fig. 3. Microscope images of 3.0 mm BVS scaffolds deployed within an in vitro silicon lesion model at 37 deg C. A) Postdilatation with 3.0 × 10 mm high pressure NC OPN balloon (SIS Medical AG, Winterthur Switzerland) (30 ATM). B) Postdilatation with 3.5 × 10 mm high pressure NC OPN balloon (30 ATM). In this model experiment, postdilatation with high pressure NC OPN balloon (limited to diameter 0.5 mm above scaffold nominal size) did not cause any BVS strut disruption. [Color figure can be viewed in the online issue, which is available at wileyonlinelibrary.com.]

suboptimal result than the targets indicated of ISA<5% and RAS <20% [17]. The minimal lumen area achieved in our study was 5.5 ± 1.4 mm^2, higher than the cut-off considered as the threshold increasing the risk of adverse events after drue eluting stent (DES) implantation [18]. Moreover, OCT has been shown to measure lower absolute areas than IVUS [19].

It is unclear whether BVS underexpansion or malapposition translates into adverse clinical outcomes, but the importance of implantation technique is suggested by the different rate of stent thrombosis according to frequency and pressure used for postdilatation. In studies and registries where postdilation was rarely used (<50% of cases with a final pressure of less than 15 atm), the rate of stent thrombosis was 2–3% [7,8]. Conversely, when routine and more aggressive postdilatation was used (99–100% of the cases with a final mean pressure of 21 atm) no scaffold thrombosis was reported [11,20]. Moreover, the vast majority of scaffold thrombosis occurred in the first 30 days after BVS implantation, suggesting the importance of procedural technical features.

The presence of focal calcium or fibrosis or a high plaque burden behind the scaffold might cause asymmetrical scaffold expansion. The use of HPPD can represent a strategy to optimize stent expansion and symmetry. Brugaletta et al. [14] reported a higher symmetry index for the BVS compared with the DES, whereas the eccentricity index was significantly lower in the BVS. In the current study, we found a slightly higher eccentricity index (0.86 vs. 0.85) and symmetry index (0.35 vs. 0.31). These results achieved in more complex lesions seem to suggest that the impact of plaque and vessel compliance on the final BVS expansion can be limited by an appropriate use of postdilation (Fig. 2). These results do not necessarily apply to simpler lesions, where the use of HPPD could be not necessary. Despite our population is represented mainly by complex lesions, our results are still relevant for the real word clinical setting because most of the lesions

encountered in everyday practice are more complex than the lesions treated in previous BVS-trials. Moreover, the use of BVS for treatment of complex lesions is increasing [7,19].

In our population of stable lesions, plaque prolapse was small and not clinically relevant as it caused only a minimal reduction of the final mean lumen area. Moreover, the thicker struts of the BVS mean that the prolapsed plaque was always surrounded by the scaffold struts with less herniation into the vessel lumen and a smoother surface compared with thinner DES struts (Fig. 1). Tissue prolapse might be more prominent in unstable or thrombus-containing lesions [21], where HPPD certainly plays a lower role.

Our study found only one edge dissection (4.5%) (not requiring further stent implantation), where the reported incidence of edge dissections range between 7.9–40% [11,17,22,23]. The fact that predilation could be performed only in the central lesion segment with short high pressure balloons, leaving to HPPD the final expansion of the BVS, may explain these results.

To our knowledge, this is also the first study describing the clinical experience of OPN NC Balloon for BVS post dilation. This high-pressure balloon with an extremely low compliance (rated burst pressure 35 atm) uses twin-layer balloon technology to ensure uniform balloon expansion (see Fig. 3 for a model experiment example of HPPD with a OPN NC balloon). Our group recently reported the safety and efficacy of OPN balloons for treatment with DES of highly resistant coronary lesions nonresponsive to conventional NC balloon inflation [24]. In devices highly sensitive to excessive volume expansion as BVS, a balloon that guarantees an extremely low growth even at 40 atm increases the safety of BVS optimization. In this sense, it has also to be noted that the choice of an appropriate balloon diameter for the scaffold diameter remains extremely important to perform HPPD safely.

To specifically address the exact role of postdilation strategy in BVS deployment further clinical studies are warranted but it will not be surprising if the "antique" practice of a postdilation could become in the near future the routine practice of scaffold deployment.

LIMITATIONS

The selection of BVS and balloon diameter in this study was guided by OCT guidance. A misjudgement of the true vessel diameter and the need of excessive over expansion of a poorly selected, too small BVS may lead to poor results. Our findings are probably valid only for conservative postdilation.

This study is a preliminary single-center study and the use of HPPD was prompted by the lack of response to conventional pressure. This selection impairs the possibility to compare these results with results obtained in simpler lesions. Still, it is clinically of interest that the percentages of RAS, ISA, and minimal lumen area are similar to those observed in lesions treated with lower pressure and reported in previous OCT studies from our center[11].

Although no new Q waves or ST-segment elevation or prolonged chest pain were observed, we did not consistently measure postprocedural troponin in all patients. Finally, this study was not designed to assess the relationship between the acute performance of BVS after high pressure and late events. Further studies are required to investigate clinical implications of OCT findings after HPPD.

CONCLUSIONS

BVS deployment optimization using HPPD with nonoversized NC balloons does not cause BVS disruption and is associated with a good BVS expansion, low strut malapposition, and edge dissection.

REFERENCES

1. Nakamura S, Colombo A, Gaglione A, Almagor Y, Goldberg SL, Maiello L, Finci L, Tobis JM. Intracoronary ultrasound observations during stent implantation. Circulation 1994;89: 2026–2034.
2. Serruys PW, Ormiston JA, Onuma Y, Regar E, Gonzalo N, Garcia-Garcia HM, Nieman K, Bruining N, Dorange C, Miquel-Hebert K, Veldhof S, Webster M, Thuesen L, Dudek D. A bioabsorbable everolimus-eluting coronary stent system (absorb): 2-year outcomes and results from multiple imaging methods. Lancet 2009;373:897–910.
3. Serruys PW, Onuma Y, Dudek D, Smits PC, Koolen J, Chevalier B, de Bruyne B, Thuesen L, McClean D, van Geuns RJ, Windecker S, Whitbourn R, Meredith I, Dorange C, Veldhof S, Hebert KM, Sudhir K, Garcia-Garcia HM, Ormiston JA. Evaluation of the second generation of a bioresorbable everolimus-eluting vascular scaffold for the treatment of de novo coronary artery stenosis: 12-month clinical and imaging outcomes. J Am Coll Cardiol 2011;58:1578–1588.
4. Ormiston JA, Serruys PW, Onuma Y, van Geuns RJ, de Bruyne B, Dudek D, Thuesen L, Smits PC, Chevalier B, McClean D, Koolen J, Windecker S, Whitbourn R, Meredith I, Dorange C, Veldhof S, Hebert KM, Rapoza R, Garcia-Garcia HM. First serial assessment at 6 months and 2 years of the second generation of absorb everolimus-eluting bioresorbable vascular scaffold: A multi-imaging modality study. Circ Cardiovasc Interv 2012;5:620–632.
5. Onuma Y, Serruys PW, Ormiston JA, Regar E, Webster M, Thuesen L, Dudek D, Veldhof S, Rapoza R. Three-year results of clinical follow-up after a bioresorbable everolimus-eluting scaffold in patients with de novo coronary artery disease: The absorb trial. EuroIntervention 2010;6:447–453.
6. Serruys PW, Onuma Y, Ormiston JA, de Bruyne B, Regar E, Dudek D, Thuesen L, Smits PC, Chevalier B, McClean D, Koolen J, Windecker S, Whitbourn R, Meredith I, Dorange C, Veldhof S, Miquel-Hebert K, Rapoza R, Garcia-Garcia HM.

Evaluation of the second generation of a bioresorbable everolimus drug-eluting vascular scaffold for treatment of de novo coronary artery stenosis: Six-month clinical and imaging outcomes. Circulation 2010;122:2301–2312.
7. Capodanno D, Gori T, Nef H, Latib A, Mehilli J, Lesiak M, Caramanno G, Naber C, Di Mario C, Colombo A, Capranzano P, Wiebe J, Araszkiewicz A, Geraci S, Pyxaras S, Mattesini A, Naganuma T, Munzel T, Tamburino C. Percutaneous coronary intervention with everolimus-eluting bioresorbable vascular scaffolds in routine clinical practice: Early and midterm outcomes from the european multicentre ghost-eu registry. EuroIntervention 2015;10:1144–1153.
8. Kraak RP, Hassell ME, Grundeken MJ, Koch KT, Henriques JP, Piek JJ, Baan J, Jr., Vis MM, Arkenbout EK, Tijssen JG, de Winter RJ, Wykrzykowska JJ. Initial experience and clinical evaluation of the absorb bioresorbable vascular scaffold (bvs) in real-world practice: The amc single centre real world pci registry. EuroIntervention 2015;10:1160–1168.
9. Di Mario C, Caiazzo G. Biodegradable stents: The golden future of angioplasty? Lancet 2015;385:10–12.
10. Tearney GJ, Regar E, Akasaka T, Adriaenssens T, Barlis P, Bezerra HG, Bouma B, Bruining N, Cho JM, Chowdhary S, Costa MA, de Silva R, Dijkstra J, Di Mario C, Dudek D, Falk E, Feldman MD, Fitzgerald P, Garcia-Garcia HM, Gonzalo N, Granada JF, Guagliumi G, Holm NR, Honda Y, Ikeno F, Kawasaki M, Kochman J, Koltowski L, Kubo T, Kume T, Kyono H, Lam CC, Lamouche G, Lee DP, Leon MB, Maehara A, Manfrini O, Mintz GS, Mizuno K, Morel MA, Nadkarni S, Okura H, Otake H, Pietrasik A, Prati F, Raber L, Radu MD, Rieber J, Riga M, Rollins A, Rosenberg M, Sirbu V, Serruys PW, Shimada K, Shinke T, Shite J, Siegel E, Sonoda S, Suter M, Takarada S, Tanaka A, Terashima M, Thim T, Uemura S, Ughi GJ, van Beusekom HM, van der Steen AF, van Es GA, van Soest G, Virmani R, Waxman S, Weissman NJ, Weisz G. Consensus standards for acquisition, measurement, and reporting of intravascular optical coherence tomography studies: A report from the international working group for intravascular optical coherence tomography standardization and validation. J Am Coll Cardiol 2012;59:1058–1072.
11. Mattesini A, Secco GG, Dall'Ara G, Ghione M, Rama-Merchan JC, Lupi A, Viceconte N, Lindsay AC, De Silva R, Foin N, Naganuma T, Valente S, Colombo A, Di Mario C. Absorb biodegradable stents versus second-generation metal stents:A comparison study of 100 complex lesions treated under oct guidance. JACC Cardiovasc Interv 2014;7:741–750.
12. Barlis P, Dimopoulos K, Tanigawa J, Dzielicka E, Ferrante G, Del Furia F, Di Mario C. Quantitative analysis of intracoronary optical coherence tomography measurements of stent strut apposition and tissue coverage. Int J Cardiol 2010;141:151–156.
13. Prati F, Guagliumi G, Mintz GS, Costa M, Regar E, Akasaka T, Barlis P, Tearney GJ, Jang IK, Arbustini E, Bezerra HG, Ozaki Y, Bruining N, Dudek D, Radu M, Erglis A, Motreff P, Alfonso F, Toutouzas K, Gonzalo N, Tamburino C, Adriaenssens T, Pinto F, Serruys PW, Di Mario C. Expert review document part 2: Methodology, terminology and clinical applications of optical coherence tomography for the assessment of interventional procedures. Eur Heart J 2012;33:2513–2520.
14. Brugaletta S, Gomez-Lara J, Diletti R, Farooq V, van Geuns RJ, de Bruyne B, Dudek D, Garcia-Garcia HM, Ormiston JA, Serruys PW. Comparison of in vivo eccentricity and symmetry indices between metallic stents and bioresorbable vascular scaffolds: Insights from the absorb and spirit trials. Catheter Cardiovasc Interv 2012;79:219–228.
15. Takarada S, Imanishi T, Liu Y, Ikejima H, Tsujioka H, Kuroi A, Ishibashi K, Komukai K, Tanimoto T, Ino Y, Kitabata H, Kubo T, Nakamura N, Hirata K, Tanaka A, Mizukoshi M, Akasaka T. Advantage of next-generation frequency-domain optical coherence tomography compared with conventional time-domain system in the assessment of coronary lesion. Catheter Cardiovasc Interv 2010;75:202–206.
16. Fujino Y, Bezerra HG, Attizzani GF, Wang W, Yamamoto H, Chamie D, Kanaya T, Mehanna E, Tahara S, Nakamura S, Costa MA. Frequency-domain optical coherence tomography assessment of unprotected left main coronary artery disease-a comparison with intravascular ultrasound. Catheter Cardiovasc Interv 2013;82:E173–E183.
17. Gomez-Lara J, Diletti R, Brugaletta S, Onuma Y, Farooq V, Thuesen L, McClean D, Koolen J, Ormiston JA, Windecker S, Whitbourn R, Dudek D, Dorange C, Veldhof S, Rapoza R, Regar E, Garcia-Garcia HM, Serruys PW. Angiographic maximal luminal diameter and appropriate deployment of the everolimus-eluting bioresorbable vascular scaffold as assessed by optical coherence tomography: An absorb cohort b trial substudy. EuroIntervention 2012;8:214–224.
18. Fujii K, Carlier SG, Mintz GS, Yang YM, Moussa I, Weisz G, Dangas G, Mehran R, Lansky AJ, Kreps EM, Collins M, Stone GW, Moses JW, Leon MB. Stent underexpansion and residual reference segment stenosis are related to stent thrombosis after sirolimus-eluting stent implantation: An intravascular ultrasound study. J Am Coll Cardiol 2005;45:995–998.
19. Gonzalo N, Serruys PW, Garcia-Garcia HM, Van Soest G, Okamura T, Ligthart J, Knaapen M, Verheye S, Bruining N, Regar E. Quantitative ex vivo and in vivo comparison of lumen dimensions measured by optical coherence tomography and intravascular ultrasound in human coronary arteries. Rev Esp Cardiol 2009;62:615–624.
20. Costopoulos C, Latib A, Naganuma T, Miyazaki T, Sato K, Figini F, Sticchi A, Carlino M, Chieffo A, Montorfano M, Colombo A. Comparison of early clinical outcomes between absorb bioresorbable vascular scaffold and everolimus-eluting stent implantation in a real-world population. Catheter Cardiovasc Interv 2015;85:E10–E15.
21. Hong YJ, Jeong MH, Ahn Y, Mintz GS, Kim SW, Lee SY, Kim SY, Cho JG, Park JC, Pichard AD, Satler LF, Waksman R, Kang JC, Weissman NJ. Incidence, predictors, and clinical impact of tissue prolapse after stent implantation for saphenous vein graft disease: Intravascular ultrasound study. Int J Cardiol 2013;168:3073–3075.
22. Gonzalo N, Serruys PW, Okamura T, Shen ZJ, Onuma Y, Garcia-Garcia HM, Sarno G, Schultz C, van Geuns RJ, Ligthart J, Regar E. Optical coherence tomography assessment of the acute effects of stent implantation on the vessel wall: A systematic quantitative approach. Heart 2009;95:1913–1919.
23. Kubo T, Imanishi T, Kitabata H, Kuroi A, Ueno S, Yamano T, Tanimoto T, Matsuo Y, Masho T, Takarada S, Tanaka A, Nakamura N, Mizukoshi M, Tomobuchi Y, Akasaka T. Comparison of vascular response after sirolimus-eluting stent implantation between patients with unstable and stable angina pectoris: A Serial Optical Coherence Tomography Study. JACC Cardiovasc Imaging 2008;1:475–484.
24. Secco GG, Ghione M, Mattesini A, Dall'Ara G, Ghilencea L, Kilickesmez K, De Luca G, Fattori R, Parisi R, Marino PN, Lupi A, Foin N, Di Mario C. Very high pressure dilatation for undilatable coronary lesions: Indications and results with a new dedicated balloon. EuroIntervention. 2015;11. pii: 20131217-09. doi: 10.4244/EIJY15M06_04.